Neutron-diffraction studies of amorphous CN_x materials

J. K. Walters
Department of Physics and Astronomy, University College London, Gower Street, London WC1E 6BT, United Kingdom

M. Kühn and C. Spaeth
Technical University Chemnitz-Zwickau, 09107 Chemnitz, Germany

H. Fischer
Institut Laue Langevin, B.P. 156, 38042, Grenoble Cedex 9, France

F. Richter
Technical University Chemnitz-Zwickau, 09107 Chemnitz, Germany

R. J. Newport
Physics Laboratory, The University, Canterbury, Kent CT2 7NR, United Kingdom
(Received 30 June 1997)

The results of neutron-diffraction experiments performed on two samples of amorphous CN_x, with nitrogen concentrations of 5 and 30 at. %, prepared by a combination of filtered cathodic arc and Kaufman-type ion source, are presented. Increasing the N content of the samples is seen to cause a decrease of the average bond length and the first coordination number. An increase in the average bond angle from 113° to 121° is also observed. The pair-distribution functions indicate that N incorporation results in some transformation of sp^3 C sites to sp^2 sites, but there is no evidence for N inducing the formation of crystalline graphitic clusters, and the overall structure remains amorphous. A direct subtraction of the two data sets emphasizes the loss of sp^3 bonds and the increasing sp^2 character of the higher-N-content sample, and shows the occurrence of a variety of bonding environments for N. More limited information on second neighbor correlations involving N is also revealed. [S0163-1829(97)04346-4]

INTRODUCTION

Carbon nitride materials have been a subject of considerable attention since the theoretical work of Liu and Cohen suggesting β-C_3N_4 as a hypothetical structure exhibiting attractive physical properties.[1] Further investigations with refined methods have shown that there are a variety of other crystalline structures, with different elemental compositions, which may have a similar structural stability.[2,3] However, only a few authors have reported the experimental synthesis of crystalline carbon nitrides[4–6] and in the majority of the studies films with nitrogen contents significantly lower than 50 at. % and with a disordered structure have been found.[7–11] It is necessary to distinguish between hydrogen-free a-CN_x films and hydrogenated a-C:N:H, the latter being obtained when using a hydrocarbon precursor; as in most chemical vapor deposition techniques.[12] Amorphous CN_x materials have interesting properties and a consequent range of potential applications—e.g., in the field of electronic materials, or wear protective coatings for magnetic storage devices.[13,14] In these cases, the nitrogen content in the films studied ranges from less than 1 at. % to about 30 at. %.

The investigation of physical properties of CN_x has covered chemical composition, microstructure, electronic, optical, and mechanical properties, but there is only limited knowledge on the atomic-scale structure. In fact, direct information on the atomic arrangement is needed for reliable interpretation of data from analysis techniques, e.g., infrared (IR), x-ray photoemission spectroscopy, or Raman spectroscopy.

Diffraction experiments provide an opportunity to obtain direct information on interatomic distances and on the average numbers of atoms in each coordination shell. Thus far, for CN_x materials these have been mainly limited to electron diffraction.[15,16] Neutron diffraction however, has the advantage that the scattering is from the nuclear centers and may be described within the first Born approximation, and that the interference function (or structure factor) derived from a neutron-diffraction experiment may be placed on an absolute scale: the data are fully quantitative. The instrument D4b (at the Institut Laue-Langevin, Grenoble, France) is ideally suited to looking at very small samples of amorphous material due to the high neutron flux and the excellent instrument stability.

We present here neutron-diffraction data collected for CN_x materials and use the information from the data to discuss the bonding environments of N within the network. Two samples have been selected, one with 5 at. % N and one with 30 at. % N, denoted CN05 and CN30, respectively. A full analysis of the data is presented, giving interatomic distances, bond angles, and coordination numbers for the two samples. The effect of N incorporation on the overall atomic-scale structure of the samples is also examined. These data are discussed in the context of previous experimental studies by other workers on similar materials.

EXPERIMENTAL DETAILS

The samples were prepared by thin-film deposition using a filtered cathodic arc. The arc discharge was operated with a cathode made from high-purity graphite; the carbon plasma

TABLE I. Preparation and compositional information on the two samples. For carbon (C^+) a mean ion energy was determined using a retarding field analyzer.

Sample	Deposition energy (eV)	N Content (at. %)	Density (gcm^{-3})	Number density (atoms $Å^{-3}$)
CN05	C^+~20	5	2.7	0.13
CN30	C^+~20; N_2^+~200	30	2.0	0.10

produced is highly ionized. A magnetic filter was used in order to separate macroparticles (of graphite) from the flux of film forming particles. Nitrogen could be incorporated into the growing film either by introducing a nitrogen gas flow into the deposition chamber, or by bombarding the substrate with a nitrogen ion beam from a Kaufman-type ion source—which proved necessary in order to obtain films with higher N contents, i.e., up to 30 at. %.[17] We have prepared two samples, one with the nitrogen gas flow only and one with the Kaufman ion source operated at 200 V beam voltage. The gas flow rates were 8 SCCM and 3 SCCM respectively, yielding a total pressure of 0.02 and 0.01 Pa. For the nitrogen supply a special gas mixture with 10% of the ^{15}N isotope was used to facilitate complementary NMR studies on the same samples. The substrates were held at room temperature by means of a water cooled substrate holder that was connected to ground potential. Ion current densities at the substrate have been measured prior to deposition for the cathodic arc plasma j_C, and the Kaufman ion source j_N; the measured values were $j_C \approx 1.5$ mA cm^{-2} and $j_N \approx 0.25$ mA cm^{-2}.

Powder samples are required for the neutron-diffraction experiments: we therefore had to remove the film from the underlying substrate, and to collect the material from 10 deposition runs. Applying a standard procedure from microelectronics technology, silicon wafers coated with photoresist were used as substrates; following film deposition the photoresist was dissolved in acetone and the CN_x material fell off the substrate as flaky powder. Repeated rinsing with high-purity acetone was carried out to ensure no residual photoresist contamination. The material from several films prepared under identical conditions was collected and after vaporizing a small volume of remaining pure acetone, the CN_x powder was left. Approximately 80 mg of each sample was obtained.

Information on the chemical composition and the mass density of the samples was inferred from elastic recoil detection analysis (ERDA) on films deposited onto silicon wafers under identical conditions. A summary of the characteristics of the two samples is given in Table I, and further data can be found in Ref. 17. ERDA yields hydrogen content values well below 1 at. %; however, when processing the neutron-diffraction data it was necessary to assume a slightly higher H content of approximately 5 at. %.

The neutron-diffraction data presented here were collected using the D4b twin-axis diffractometer[18] at the reactor source at the Institut Laue Langevin, Grenoble (France). The scattered-neutron intensity is measured using a pair of 64 wire proportional ^3He detectors scanning a scattering angle range from $2\theta = 3° - 138°$. The incident neutron wavelength, as determined from a nickel standard calibrant, was 0.7026 Å, which gives a corresponding Q range of 0.47–16.7 $Å^{-1}$ (the data are truncated by a small amount during the analysis procedure to 14.5 $Å^{-1}$ due to the polynomial fitting). This instrument was chosen because of its excellent stability and the high neutron flux generated by the reactor source, which is especially important for these samples because at ~80 mg they are extremely small. The powder samples were held in a thin walled vanadium can with a diameter of 5 mm. For each experiment measurements are required for the sample, the empty sample container, a background without sample or container, and a vanadium rod of comparable geometry to the sample and container. The vanadium rod measurement allows the sample scattering to be put on an absolute scale, since vanadium has a well-known, and almost entirely incoherent, scattering cross section.[19]

In a neutron-scattering experiment the aim is to determine a structure factor $S(Q)$, by measuring the differential scattering cross section

$$\frac{d\sigma}{d\Omega} \propto S(Q). \tag{1}$$

$Q = |\mathbf{Q}| = |\mathbf{k}_i - \mathbf{k}_j|$ is the wave vector transfer associated with the diffraction experiment—for elastic scattering $Q = (4\pi/\lambda)\sin\theta$, where 2θ is the scattering angle and λ is the neutron wavelength. For an amorphous material (i.e., an isotropic scatterer)[19] we then define the pair correlation function $g(r)$, where

$$g(r) = 1 + \frac{1}{2\pi^2 r\rho} \int_0^\infty Q[S(Q) - 1]\sin(Qr)dQ. \tag{2}$$

ρ is the average number density of atoms in the material and $g(r)$ is a measure of the atomic density at a distance r from a given origin atom. The pair correlation function may be obtained by Fourier transformation of the structure factor, which is directly related to the measured neutron-scattering intensity. For a binary system such as CN_x, there are contributions to the total structure factor from each atom-type pair, i.e., there are three independent contributions that are weighted to give the total structure factor. The total pair distribution function $G(r)$ is a weighted combination of the partial pair distribution functions and is defined (according to the Faber-Ziman formalism[19]) as

$$G(r) = \frac{\sum_{\alpha\beta} [c_\alpha c_\beta b_\alpha b_\beta g_{\alpha\beta}(r)]}{\left(\sum_\alpha c_\alpha b_\alpha\right)^2}, \tag{3}$$

where c_α is the atomic fraction, and b_α the coherent scattering length, respectively, of element α; and where $g_{\alpha\beta}(r)$ represents the partial terms in $G(r)$ and describes the probability of finding an atom of type β at a distance r from an atom of type α at the origin. The normalized weighting coefficients for the partial pair-correlation functions are given in Table II.

Several corrections need to be applied to the raw diffraction data before a structure factor can be generated. The major corrections are for background, container, and multiple scattering,[20] attenuation,[21] and the effects of inelastic

TABLE II. Normalized weighting coefficients for the partial structure factors and pair correlation functions [see Eq. (3)]. Units for b are fm, $c_C+c_N=1$.

Sample	C—C	C—N	N—N
CN05	0.870	0.126	0.004
CN30	0.397	0.500	0.158

scattering.[22] Details of the correction procedure for the data presented here are given in Ref. 23. For these two samples it was found that the inelastic contribution to the scattering was small and could be corrected simply by fitting a low order polynomial through the data. The source of the inelastic scattering is the small amount of hydrogen in the samples: for the purposes of the data analysis a H content of 5 at. % was assumed for both samples. Also, when Fourier transforming the structure factor to obtain the pair-correlation function, an $r_{\min}$ cutoff was applied. This is a variation on Fourier filtering in which a distance $r_{\min}$ is defined as the shortest bond length that is physically reasonable and it determines the start of correlation features in the $G(r)$.[24] From the pair-distribution function $G(r)$, we obtain the radial distribution function $J(r)$, where

$$J(r)=4\pi r^2\rho G(r), \tag{4}$$

which is a measure of the number of atoms at a given radial distance. $J(r)$ can then be fitted with a series of Gaussians, allowing position and area to vary and by this method accurate values for the bond lengths and coordination numbers can be obtained.

RESULTS AND DISCUSSION

Figures 1 and 2, respectively, show the total structure factors and pair-correlation functions obtained from the neutron-diffraction experiments, for the two samples described above.

Looking first at the $S(Q)$ data, there are some obvious differences between the two data sets. At ~ 2 Å^{-1} the shoulder that is apparent in the data for sample CN05, becomes a well-defined peak for the higher N content sample CN30. However, the emergence of a peak at this position is accompanied by a decrease in intensity of the next peak at ~ 3.5 Å^{-1}. The change in the relative intensities of these two peaks with N concentration implies that the nature of the short-range bonding in the network changes when more N is incorporated. Although it is not possible to make specific bond assignments to this Q-space data, these changes may be due to the increased sp^2 nature of the CC bonding in the higher N content sample, which is seen in the real-space data and will be discussed shortly. For both samples the main peak in the data is at ~ 5.3 Å^{-1}. From 5 at. % N to 30 at. % N this peak shows a small shift in position towards a higher Q value, together with an increase in width and a small decrease in height. More subtle changes can be seen in the series of double peaks in the region $\sim 7-12$ Å^{-1}. As the N content is increased, the first of these peaks becomes smaller, whereas the second shows an increase in relative intensity. There is also a small shift in the positions of both peaks towards higher Q values in the data for CN30. Finally, at the end of the range of the data, there is a partial peak that looks to be at a higher Q value in the higher N content sample. For sample CN30 it also appears that the intensity of this peak is lower. The data presented here should be compared to those of Gilkes *et al.*[25] for filtered cathodic arc-deposited *ta*-C, collected at the ISIS pulsed neutron source (Rutherford Appleton Laboratory, UK). The features in the *ta*-C data are similar to those seen in CN05, although the first two peaks are sharper, which is consistent with the highly ordered tetrahedral network in the *ta*-C material.

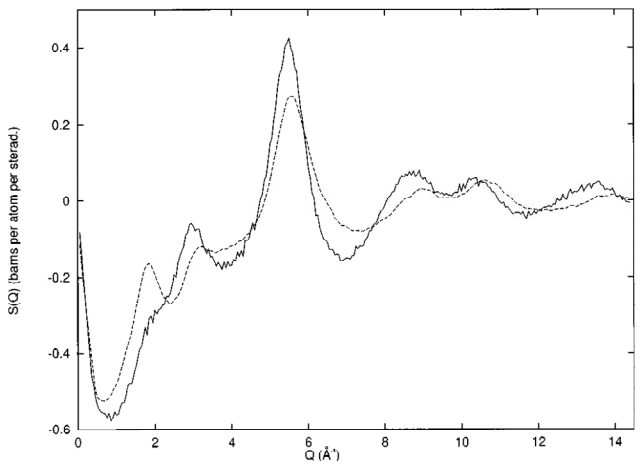

FIG. 1. The total structure factors, $S(Q)$, for the two samples obtained after correction of the neutron diffraction data: CN05 (solid line) and CN30 (dashed line).

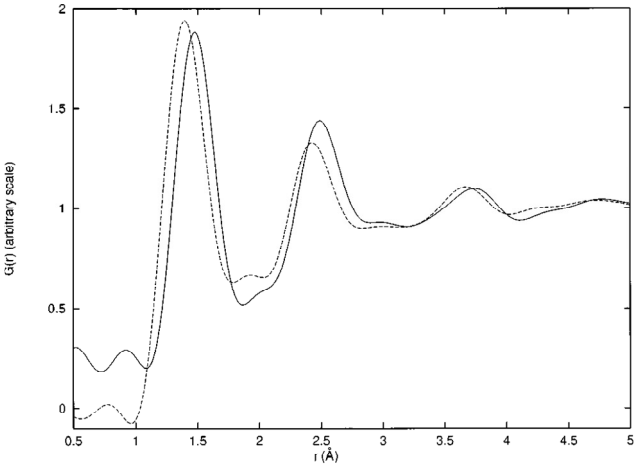

FIG. 2. The total pair correlation functions $G(r)$, for the two samples obtained by Fourier transformation of the total structure factors: CN05 (solid line) and CN30 (dashed line).

Although the differences between the $S(Q)$ data for our two samples are large, it is necessary to look at the Fourier transformed data, $G(r)$ in order to understand what they mean in terms of structural changes.

The $G(r)$ data in Fig. 2 shows three features at ~ 1.5, ~ 2.5, and ~ 3.7 Å and a broad peak centered at ~ 4.7 Å. Precise peak positions are obtained from Gaussian fitting to the radial distribution functions $J(r)$, which are shown in Fig. 3, together with the Gaussian components used to obtain the fit. The bond lengths and coordination numbers determined from the Gaussian fitting are given in Table III. All

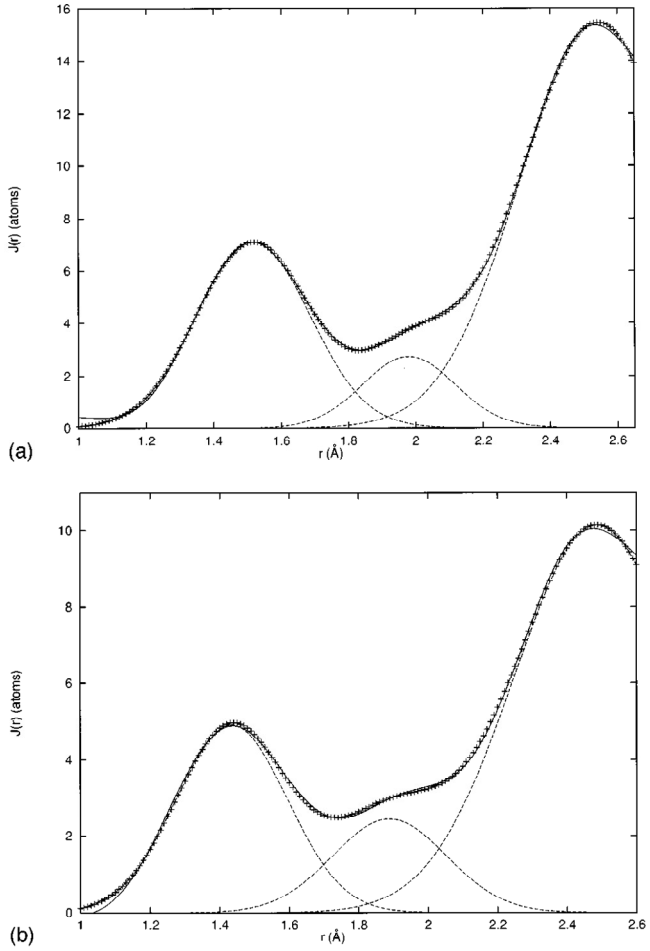

FIG. 3. The total peak fits (+) to the experimentally derived radial distribution function $J(r)$, for sample CN05 (a) and sample CN30 (b), showing the Gaussian components (----).

three of the main $G(r)$ peaks show a shift in position towards lower r values for CN30 compared to CN05, and this is reflected quantitatively in the results shown in Table III. The average first-neighbor distance, for example, is 1.52 Å in CN05 and is 1.43 Å for CN30. However, note that within the experimental errors, the width of this first peak remains constant. A similar shift in nearest-neighbor distance has been observed by Davis *et al.*[15] in electron diffraction from CN_x films prepared by filtered cathodic arc deposition: at 1% dopant concentration the distance was found to be 1.54 Å, compared to 1.43 Å at 15% dopant concentration. To some extent, this shift to shorter average bond lengths is simply due to the incorporation of CN bonds in the network—on average these are shorter than CC bonds. Note that we mentioned previously the possibility of the samples being contaminated with up to 5 at. % H. This would result in features in the $G(r)$ at 1.1 Å (C—H, negative) and at ~1.8 Å (CCH, negative and HCH, positive). In neutron-diffraction data for a-C:N:H samples containing ~20 at. % H (Ref. 26), a clear, sharp dip at 1.1 Å can be seen, however the second-neighbor correlations at ~1.8 Å are broad and undefined. In the data presented here for amorphous CN_x samples, there is no evidence for C—H bonds at 1.1 Å, which implies that the H contamination is too small to give an observable contribution to the $G(r)$ distribution. Also, since this first-neighbor feature is usually stronger than those for second neighbors, we can conclude that contributions to the $G(r)$ from CCH and HCH correlations will be negligible. Therefore, the data in Fig. 2 and the conclusions drawn from it will be unaffected by H contamination of the samples.

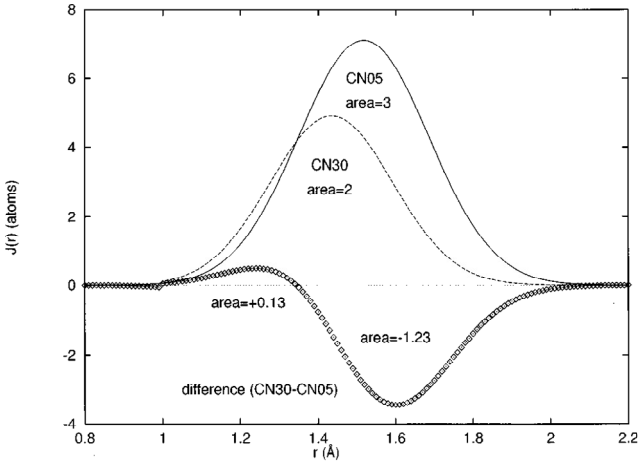

FIG. 4. The difference $J(r)$, evaluated from the subtraction of the first two fitted Gaussian peaks for the samples, CN05-CN30.

For further evaluation of the structural differences between sample CN05 and CN30, the first Gaussian fitted to each of the $J(r)$ functions was taken as a measure of the first coordination sphere. The difference between these two distributions comprises information on changes in bonding configurations, i.e., negative features are associated with bond types that are removed when 30 at. % N is added, whereas any increase in bond types will generate positive features in the difference function. Figure 4 shows the shape of the difference function and the areas of the negative and positive contributions. It should be noted that differences due to CC bonds replaced by CN bonds with similar bond lengths are not visible, since the resolution of the data means that it is not possible to distinguish between the elements. Thus, in the CN30 sample there are significantly fewer first-neighbor atoms with bond lengths typical for sp^3 carbon bonds than in

TABLE III. Results of the Gaussian fitting of the radial distribution function, $J(r)$.

Sample	N content (at. %)	First neighbor peak position (±0.01 Å)	First neighbor peak area ±20% (atoms)	Second neighbor peak positions (±0.01 Å)	Average CCC bond angle (±2°)
CN05	5	1.52	3	1.98 2.54	113
CN30	30	1.43	2	1.89 2.49	121

TABLE IV. Some of the tabulated bond distances for carbon and nitrogen in organic compounds (Ref. 41).

C—C	Diamond	1.54 Å
C≈C	Graphite	1.42 Å
C≈C	Benzene	1.399 Å
C═C	Ethene	1.34 Å
C≡C	Acetylene	1.203 Å
C—N	Aziridine	1.47 Å
C═N	Pyrazole	1.33 Å
C═N	Furazan	1.30 Å
C≈N	Pyridine	1.34 Å
C≡N		1.14 Å
N—N	Pyrazole	1.37 Å
N≈N	Pyridazine	1.30 Å
N═N		1.24 Å
N═N	Azides	1.12 Å

the CN05 sample. In the region below ~1.35 Å, a slightly higher number of bonds is observed for CN30 than in CN05. Clearly, this is attributed to the presence of various types of CN bonds. Table IV gives some of the tabulated values for CN, CC, and NN bonds. At distances below ~1.35 Å, possible contributions could be from C≡N (~1.14 Å), C═N (~1.30 Å), and aromatic C≈N (~1.30–1.36 Å) bonds. Also, further possibilities are sp^1 C≡C (~1.18 Å) and N═N (~1.24 Å) configurations, although there is only a small probability that these will occur. It would also be reasonable to assume the existence of C—N single bonds (~1.35–1.39 Å), although these cannot be resolved because of their similarity to sp^2 CC bond distances. In experimental data for other CN_x samples,[27–29] sp^1 C≡C bonds have not been observed, so we may assume that they are probably not present in our samples in significant numbers. This leads us to conclude that sample CN30 contains significant numbers of C═N and C≡N bonds. Both types of bonds have been observed in other experimental data,[29–33] as have C—N; however until now, it has not been possible to determine the relative numbers of each bonding type since fully quantitative data is required.

These results show that adding N to the network not only creates CN bonds, but also precipitates a conversion of sp^3 C—C bonds to (olefinic/graphitic) sp^2 C═C bonds. This change is also apparent when we consider the average bond angles given in Table III. There is a considerable change in bond angle in going from 5 at. % N to 30 at. % N. At the low N concentration, the CCC bond angle is 113°, which is similar to values obtained by Davis *et al.*[15] for 1% N doping. For *ta*-C, values of ~109° are observed.[16,25] At 30 at. % N (sample CN30), the average CCC bond angle is 121°, which is close to the value in crystalline graphite (120°) and the same as that for 15% N dopant concentration.[15] A similar effect has also been observed in the hydrogenated *a*-C:N:H material.[26] Indeed, there is now much experimental evidence to support the claim that doping with N induces a change in the CC bonding character to be more graphitic (see, for example, Refs. 15, 16, 30, 34–36).

We now focus on the nature of the disorder in the structure. From Fig. 3, the widths of the near neighbor peaks for CN05 and CN30 are the same, but there is an increase in intensity in the high N content sample at ~2.0 Å, between the first two main peaks. This is also observed in electron-diffraction data.[15] A peak at this distance will be due to second-neighbor correlations, although a specific assignment is not possible. Therefore, the following discussion on the origins of this feature is necessarily speculative.

As we have seen, the addition of 30 at. % N not only introduces CN bonds into the network, but also causes the CC bonding environment to change from sp^3 C—C to predominantly sp^2 C≈C, which makes it more difficult to pinpoint the source of this "intermediate" peak. If we use a first-neighbor distance of 1.2 Å, then the bond angle for this intermediate distance comes out at 112°. If we use a first-neighbor distance of 1.43 Å, this gives a bond angle of 89°, and halfway between the two first-neighbor distances results in a bond angle of 99°. These three first-neighbor distances correspond to NCN, CCC, and NCC correlations, respectively. Since we have already established that the dominant bonding environments for N are C≡N and C═N, then we expect that there will be few NCN correlations in the network. Also, 89° is far too small a bond angle for physically reasonable CCC correlations, and we know from other diffraction data[26,37] that the peak at ~2.5 Å is assigned to CCC second-neighbor distances. This leaves NCC correlations. The bond angle is smaller than would be anticipated, but is perhaps more reasonable given the strained nature of the network structure.[34,38] Recently, Marks *et al.*[39] have published theoretical studies giving four-membered rings with bond angles around 90°, for which evidence from organic chemistry is used. However, the chemical ring formations cited, namely, cyclobutane and cyclopentane, are both hydrogenated systems. Another possibility is that this correlation feature at ~2.0 Å arises from three atoms which are not all connected, e.g., a dangling N from C≡N bond close to another C atom. In this example, only two of the three atoms in the CNC bond angle are actually bonded, but the three atoms together produce a second-neighbor distance of ~2.0 Å and a corresponding bond angle ~90°. The addition of N is reported to affect the void structure of the material,[24] and it is feasible that this or a similar atomic arrangement could arise.

From the results of the Gaussian fitting in Table III we may also obtain peak areas, which correspond to the average coordination numbers. These values can only be discussed meaningfully for the first coordination shell because of the mixture of second-neighbor correlations noted above. For CN05 the average first coordination number is $3 \pm 20\%$, whereas for CN30 it has been reduced to $2 \pm 20\%$. These results should be compared to the value of 3.9 for *ta*-C obtained by Gilkes *et al.*[25] Also, for CN05 we can use a method described by Ref. 25, where the coordination number is calculated from the average first-neighbor bond length. Ignoring the contributions of CN bonds, we obtain a first coordination number of 3.8 for CN05. Although this is only a zero-order approach, it does indicate that the value determined from the Gaussian peak fitting underestimates the coordination number. (One possible explanation for this is the normalization of the data to the number of scattering centres in the beam, i.e., the sample packing density. This is estimated using a simple "mass of sample/volume occupied in the can" calculation and could account for the 20% normalization error.

This error will be the same for both samples.) However, the changes observed in coordination number between the two samples still hold, as both values will be affected in the same way. It is immediately apparent that, within the experimental errors, the addition of only 5 at. % N causes a reduction in the coordination number compared to the undoped material. It is no surprise then that at 30 at. % N there is a further drop in the average coordination number to just $2 \pm 20\%$. This decrease in the coordination number fits in well with our finding that the dominant bonding environments for the incorporated N are C≡N and C═N: for C≡N, $N_N = 1$ and $N_C = 2$, and for C═N, $N_N = 2$ and $N_C = 2$ or 3 (where N_N and N_C are the coordination numbers of the N and C atoms, respectively). Thus, if the average coordination number of any atom is $2 \pm 20\%$, threefold-coordinated C atoms giving rise to the graphite bond angles are also possible.

CONCLUSIONS

The structure of two CN_x samples with 5 at. % and 30 at. % N has been investigated using neutron diffraction. From this experimental data it is possible to determine average values for bond lengths, bond angles, and coordination numbers. The data for CN05 yield 1.52 Å, 113°, and three atoms, respectively. Comparing this to the data for *ta*-C (Ref. 25) it is shown that the incorporation of nitrogen induces structural changes, in particular, a significant reduction of the coordination number. Further addition of N to the network (sample CN30) is found to reduce the number of sp^3 C—C bonds, while increasing the number of olefinic/graphitic sp^2 C═C bonds. The average values for bond length, bond angle, and coordination number are 1.43 Å, 121°, and two atoms.

The differences between the structure of sample CN05 and CN30 have been evaluated by subtracting the two data sets. It is clear that for CN30 a different variety of bonding types at bond lengths below 1.35 Å appears. At this point, it is not possible to obtain more conclusive information on the relative amount of specific bonding types (i.e., C≡N, C═N, etc.) and therefore the results from other analysis techniques, e.g., NMR and IR spectroscopy, need to be included. Alternatively, comparison with model structures obtained by computer simulation (using the methods of Ref. 40) may give further insight into atomic arrangements that are compatible with the diffraction data presented here.

ACKNOWLEDGMENTS

J.K.W. acknowledges the generous financial support of the Royal 1851 Commission and the Royal Society. The project was also sponsored by the Bundesministerium für Bildung, Wissenschaft, Forschung und Technologie under Grant No. 03 N 5002 C. We are grateful to the ILL for providing access to their neutron research facilities, particularly P. Palleau for technical assistance with the measurements, and to Th. Frauenheim for catalyzing this collaborative endeavor.

[1] A. Y. Liu and M. L. Cohen, Phys. Rev. B **41**, 10 727 (1990).
[2] D. M. Teter and R. J. Hemley, Science **271**, 53 (1996).
[3] M. Côté and M. L. Cohen, Phys. Rev. B **55**, 5684 (1997).
[4] K. M. Yu, M. L. Cohen, E. E. Haller, W. L. Hansen, A. L. Liu, and I. C. Wu, Phys. Rev. B **49**, 5034 (1994).
[5] X. W. Su, H. W. Song, F. Z. Cui, and W. Z. Li, J. Phys. E 7, 517 (1995).
[6] Y. Chen, L. Guo, and E. G. Wang, Philos. Mag. Lett. **75**, 155 (1997).
[7] C. A. Davis, D. R. McKenzie, Y. Yin, E. Kravtchinskaia, G. A. J. Amaratunga, and V. S. Veerasamy, Philos. Mag. B **69**, 1133 (1994).
[8] K. J. Boyd, D. Marton, S. S. Todorov, A. H. Al-Bayati, J. Kulik, R. A. Zuhr, and J. W. Rabalais, J. Vac. Sci. Technol. A **13**, 2110 (1995).
[9] D. Li, E. Cutiongco, Y.-W. Chung, M.-S. Wong, and W. D. Sproul, Diamond Films Technol. **5**, 261 (1995).
[10] Z. J. Zhang, J. Huang, S. Fan, and C. M. Lieber, Mater. Sci. Eng. A **209**, 5 (1996).
[11] H. Sjöström, L. Hultman, J.-E. Sundgren, and S. V. Hainsworth, J. Vac. Sci. Technol. A **14**, 56 (1996).
[12] F. L. Freire, G. Mariotto, C. A. Achete, and D. F. Franceschini, Surf. Coat. Technol. **74/75**, 382 (1995).
[13] J. Robertson and C. A. Davis, Diamond Relat. Mater. **4**, 441 (1995).
[14] E. C. Cutiongco, D. Li, Y.-W. Chung, and C. S. Bhatia, J. Tribology **118**, 543 (1996).
[15] C. A. Davis, Y. Yin, D. R. McKenzie, L. E. Hall, E. Kravtchinskaia, V. Keast, G. A. J. Amaratunga, and V. S. Veerasamy, J. Non-Cryst. Solids **170**, 46 (1994).
[16] A. R. Merchant, D. G. McCulloch, D. R. McKenzie, Y. Yin, L. E. Hall, and E. G. Gerstner, J. Appl. Phys. **79**, 6914 (1996).
[17] C. Spaeth, M. Kühn, U. Kreissig, and F. Richter, Diamond Relat. Mater. **6**, 626 (1997).
[18] K. Ibel (unpublished); for recent information on ILL facilities, see http://www.ill.fr/
[19] R. J. Newport, in *Neutron Scattering at a Pulsed Source*, edited by R. J. Newport, B. D. Rainford, and R. Cywinski (Hilger, Bristol, 1988), p. 233.
[20] A. K. Soper and P. A. Egelstaff, Nucl. Instrum. Methods **178**, 415 (1980).
[21] H. H. Paalman and C. J. Pings, J. Appl. Phys. **33**, 2635 (1962).
[22] G. Placzek, Phys. Rev. **86**, 377 (1952); A. K. Soper and A. Lazar, J. Chem. Phys. **97**, 1320 (1992).
[23] After the method of A. K. Soper, W. S. Howells, and A. C. Hannon, Rutherford Appleton Laboratory Report No. RAL-89-046, 1989 (unpublished).
[24] A. K. Soper in *Neutron Scattering Data Analysis 1990*, edited by M. W. Johnson (IOP, Bristol, 1990), p. 57.
[25] K. W. R. Gilkes, P. H. Gaskell, and J. Robertson, Phys. Rev. B **51**, 12 303 (1995); K. W. R. Gilkes, P. H. Gaskell, and J. Yuan, J. Non-Cryst. Solids **164-166**, 1107 (1993).
[26] J. K. Walters, R. J. Newport, W. S. Howells, and G. Bushnell-Wye, J. Phys. Condens. Matter **8**, 4739 (1996).
[27] H. Han and B. J. Feldman, Solid State Commun. **65**, 921 (1988).
[28] T. Okada, S. Yamada, Y. Takeuchi, and T. Wada, J. Appl. Phys. **78**, 7416 (1995).
[29] J. H. Kaufman and S. Metin, Phys. Rev. B **39**, 13 053 (1989).
[30] F. Rossi, B. Andre, A. van Veen, P. E. Mijnarends, H. Schut, F. Labohm, M. P. Delplancke, H. Dunlop, and E. Anger, Thin Solid Films **253**, 85 (1994).

[31] M. Friedrich, Th. Welzel, R. Rochotzki, H. Kupfer, and D. R. T. Zahn, Diamond Relat. Mater. **6**, 33 (1997).
[32] D. Lin, S. Lopez, Y. W. Chung, M. S. Wong, and W. D. Sproul, J. Vac. Sci. Technol. A **13**, 1063 (1995).
[33] J. Schwan, W. Dworschak, K. Jung, and H. Ehrhardt, Diamond Relat. Mater. **3**, 1034 (1994).
[34] G. A. J. Amaratunga, V. S. Veerasamy, C. A. Davis, W. I. Milne, D. R. McKenzie, J. Yuan, and M. Weiler, J. Non-Cryst. Solids **164-166**, 1119 (1993).
[35] V. S. Veerasamy, J. Yuan, G. A. J. Amaratunga, W. I. Milne, K. W. R. Gilkes, M. Weiler, and L. M. Brown, Phys. Rev. B **48**, 17 954 (1993).
[36] S. R. P. Silva, B. Rafferty, G. A. J. Amaratunga, J. Schwan, D. F. Franceschini, and L. M. Brown, Diamond Relat. Mater. **5**, 401 (1996).
[37] J. K. Walters, P. J. R. Honeybone, D. W. Huxley, R. J. Newport, and W. S. Howells, Phys. Rev. B **50**, 831 (1994).
[38] D. F. Franceschini, C. A. Achete, and F. L. Freire, Appl. Phys. Lett. **60**, 3229 (1992).
[39] N. A. Marks, D. R. McKenzie, B. A. Pailthorpe, M. Bernasconi, and M. Parinello, Phys. Rev. B **54**, 9703 (1996).
[40] G. Jungnickel, M. Kühn, S. Deutschmann, F. Richter, U. Stephan, P. Blaudeck, and Th. Frauenheim, Diamond Relat. Mater. **3**, 1056 (1994).
[41] *CRC Handbook of Chemistry and Physics 75th Ed.*, edited by D. R. Lide and H. P. R. Frederikse (CRC, Boca Raton, 1994).